Journal of Solid Mechanics Vol. 12, No. 4 (2020) pp. 829-846
DOI: 10.22034/jsm.2019.1879783.1504

Tangential Displacement and Shear Stress Distribution in Non-Uniform Rotating Disk under Angular Acceleration by Semi-Exact Methods

S. Jafari *

Department of Mechanical Engineering, University of Bojnord, Bojnord, Iran

Received 21 July 2020; accepted 23 September 2020

ABSTRACT

In this paper, semi-exact methods are introduced for estimating the distribution of tangential displacement and shear stress in non-uniform rotating disks. At high variable angular velocities, the effect of shear stress on Von Mises stress is important and must be considered in calculations. Therefore, He's homotopic perturbation method (HPM) and Adomian**'s** decomposition method (ADM) is implemented for solving equilibrium equation of rotating disk in tangential direction under variable mechanical loading. The results obtained by these methods are then verified by the exact solution and finite difference method. The comparison among HPM and ADM results shows that although the numerical results are the same approximately but HPM is much easier, straighter and efficient than ADM. Numerical calculations for different ranges of thickness parameters, boundary conditions and angular accelerations are carried out. It is shown that with considering disk profile variable, level of displacement and stress in tangential direction are not always reduced and type of changing the thickness along the radius of disk and boundary condition are an important factor in this case. Finally, the optimum disk profile is selected based on the tangential displacement-shear stress distribution. The presented algorithm is useful for the analysis of rotating disk with any arbitrary function form of thickness and density that it is impossible to find exact solutions.

Keywords: Non-uniform thickness and density disk; Homotopic perturbation method; Adomian's decomposition method; Shear stress; Optimum profile.

1 INTRODUCTION

A ROTATING disk is an important structural component in varied engineering machinery and systems as gas turbine engines, gears, flywheel systems, turbo pumps, turbo generators, and centrifugal compressors turbo and flywheel [1-4]. The angular velocity of rotating disk is always constant during normal work. But with increasing applications of machiniery with high variable angular velocity, it will change over the time and the disk may have an

*Corresponding author. Tel.: + 98 583 22801111
E-mail address: s.jafari@ub.ac.ir (S. Jafari).

angular acceleration during the start or stop process of the machine and can have significant effects on the strength and safety of the disks. For example, in the starting process of centrifugal compressors, turbo until it reaches steady state, disks and rotating parts are under angular acceleration producing tangential displacement and shear stress as well as radial and tangential stresses. If the shear stress goes beyond permissible limits, it can have damaging effects on the disk and related components. Obviously, they will have influences on the displacements and stresses distributions in rotating disk. Therefore, studies of rotating circular disks with angular accelerations as mechanical loading are necessary for achieving optimal design specifications and to reduce the overall weight and costs, particularly in aerospace industry. As an example, one of the applications of studying tangential displacement-shear stress distributions is estimation of best thickness parameter having optimum and minimum shear stress and tangential displacement. Other important application of studying rotating disk under angular acceleration is correct prediction of equivalent von Mises stress. The von Mises equivalent stress is used as a criterion for determining the elastic limit angular acceleration. Elastic limit angular acceleration (ω_e^*) are occurs when the von Mises stress as equivalent stress reaches to yield strength of the material of disk. For rotating disks that are in plane stress conditions, von Mises stress as a criterion for initiating plastic deformations are calculated based on the following relationship:

$$\sigma_{eq} = \sqrt{\sigma_r^2 + \sigma_\theta^2 - \sigma_r \sigma_\theta + 3\tau_{r\theta}^2}$$

In this relation, σ_r and σ_θ are radial and tangential components of the normal stresses, $\tau_{r\theta}$ is the in-plane shear stress and σ_{eq} is equivalent von Mises stress. It is known that if tangential deformation is eliminated (angular acceleration are zero), von Mises stress is obtained from the following equation. In this case the radial and tangential stresses are the principal stresses.

$$\sigma_{eq} = \sqrt{\sigma_r^2 + \sigma_\theta^2 - \sigma_r \sigma_\theta}$$

Most of research work in the field of rotating disk is focused on the finite element simulations and numerical solutions of rotating disks with uniform and specifically variable thickness and density under constant angular velocity [1-20]. The elastic solution of rotating disks with uniform thickness can be found in many standard and advanced textbooks [21-24]. As a previous research shows, numerical methods are not very accurate and sometimes have high error rates. Finite element solutions also require commercial software and are costly. Based on the need for high precision solutions, to the knowledge of author no research work has been presented for analysis of mechanical behavior in a rotating disk under angular acceleration loading with semi-exact methods. Therefore in this paper, for the first time HPM and ADM are used to obtaining displacement-stress distribution in tangential direction of rotating disk. The proposed algorithm that included this semi-exact method can successfully handle the problem of a rotating disk in general form (any type of thickness and density function) under mechanical loading and could be extended to analysis more complicated problems of combined loading cases such as thermo-mechanical loadings. Generally, analysis of actual engineering problems includes solution of nonlinear differential equations. These differential equations cannot be solved clearly and usually attempts to find their exact solution fails. One of the well-known methods for solve these differential equations is Perturbation method (PM). This method is based on the existence of perturbation quantity for solves these problems. In order to overcome the problems associated with finding the small parameter, different new methods have been proposed to eliminate the small parameter, For example, the homotopic perturbation method [25-29] and Adomian's decomposition method (ADM) [30-32]. Homotopy perturbation method yields a very rapid convergence of the solution series in the most cases [25-29]. Adomian proposed a new method for solving linear and nonlinear equations. In this method the solution of a functional equation is considered as the sum of an infinite series which converges rapidly to the accurate solutions [30-32]. One of the first researchers to work on the theoretical treatment of elastic-plastic rotating disks is Gamer [1] and after that this researches continues in different aspects to this day [1-19]. Gamer presented exact solution for the elastic–plastic response of a rotating solid disk with uniform thickness. Following on Gamer works; the fully plastic state of solid disk with variable thickness was investigated by Guven [2-4]. Eraslan carried out numerical studies on the elastic-plastic mechanical behavior of annular disks with different thickness profiles including hyperbolic, exponential and power forms under different boundary conditions [5-9]. Hojjat et al. also have done a variety of researches on rotating disks [10-15]. They studied the elastic behavior of rotating disks by variational iteration method [10], variable material property method [11], Adomian's decomposition [12] and homotopic perturbation methods [12]. In these researches thickness and density function is considered non-uniform

and after verifying process, parametric studies are done for different value of thickness and density parameters [10-12].They presented plastic analysis of rotating disks by assuming linear strain hardening model for material behavior in plastic region by HPM [13] and variable material property method [12]. In all of these researches constant mechanical loading are imposed to rotating disks. Hojjati et al. considered functionally graded rotating disks subjected to thermo-mechanical loadings by variable material properties, Runge–Kutta's and finite element methods [14]. In optimization field, Jafari et al. presented classical and modern optimization methods in minimum weight design of elastic rotating disk with variable thickness and density. They have used Karush-Kuhn-Tucker, simulated annealing (SA) and particle swarm methods (PSO) and found that performance of PSO and SA methods are simpler and supply more flexibility [15]. Among the latest researches, Alashti et al. studied plastic behavior of a rotating disk with non-uniform thickness under constant angular velocity by considering the ductile damage models in simulations [16]. Zheng et al. presented stress analysis in functionally graded rotating disks with non-uniform thickness and variable angular velocity by finite difference method [17]. Newly, Thermo-elastic analysis of a functionally graded rotating hollow circular disk with variable thickness and angular velocity are done by Salehian et al. by galerkin method [18].Shlyannikov et al. is focusing on the crack growth rate for rotating disk in gas turbine engine compressor based on the nonlinear fracture mechanics [19]. Nayak et al. is employed variational iteration method for elastic-plastic analysis of thermo-mechanically loaded FGM disks [20].

As a result of this introduction, can stated that in a large number of studies, the assumption is that the angular velocity is constant. Because of the importance of variable angular velocities on one hand and the accuracy of semi-exact solution on other hand, tangential displacement and shear stress distributions is studied in this paper by HPM and ADM for boundary conditions that exits in real work environments. The results are compared with the exact solution for uniform disk and the results of non-uniform disk are verified by finite difference method. The optimal solution method among the HPM and ADM based on the computational time, size and cost are selected. This result can be used in the analysis of plastic deformations. The material is assumed to follow an elastic-strain hardening behavior with von Mises yield criterion. Therefore, the angular acceleration has been selected to limit the maximum stress below the yield limit of the material. Finally, parametric study is done for different ranges of thickness parameters, boundary conditions and angular accelerations. Also, the optimum thickness parameter having minimum shear stress and tangential displacement is selected. The material of the disk is considered as Inconel-718 alloy that is having density varying according to special function along the radius of the disk. The disk is assumed to be different boundary conditions:

- Radially constrained-free at the inner and outer surfaces of disk: In this case the disk with new thickness and density function are considered under angular acceleration.
- Radially constrained-guided at the inner and outer surfaces of disk: in this case for the first time the disk with this boundary condition are studied under angular acceleration.

As shown in Fig.1, in each of these boundary conditions, the angular acceleration is transmitted from the rigid shaft to the annular disk.

Fig.1
a) Radially constrained-guided. b) Radially constrained-free.

2 DISK THICKNESS PROFILE AND MATERIAL PROPERTIES

The disk is symmetric with respect to the mid plane and its profile is assumed to vary as a function of radius (r) [1,2]:

$$h(r)=h_0(\frac{r}{r_e})^{\alpha} \tag{1}$$

where α is geometric parameters ($-1\le\alpha\le1$), r_e is the outer radius of the disk and $h_\circ$ is the thickness of the disk at $r=r_e$. In Eq. (1), the thickness of disk decreases parabolically with increasing in the radius of disk when $-1\le\alpha\langle0$. If $0\langle\alpha\le1$ is considered, the thickness of disk varies linearly in radial direction. For $\alpha=0$ the thickness of disk along the radius is constant. The disk thickness variations for different values of α are shown in Fig. 2.

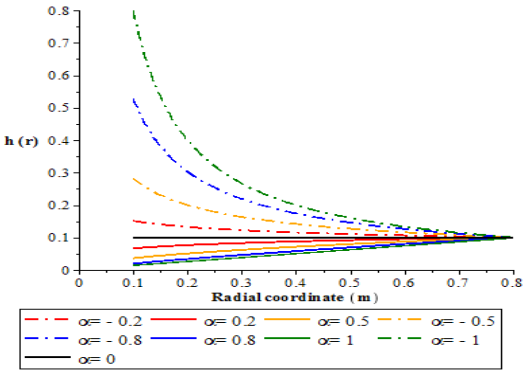

Fig.2
Disk profile for different thickness parameter α.

The material of the disk is selected as Inconel-718 having density varying according to Eq. (2). The material with this kind of continuous density change can be considered as functionally graded material (FGM).

$$\rho(r)=\rho_0+\rho_1 r+\rho_2 r^2+\rho_3 r^3 \tag{2}$$

where, $\rho_0=7800\frac{kg}{m^3},\rho_1=10\frac{kg}{m^4},\rho_2=100\frac{kg}{m^5},\rho_3=1000\frac{kg}{m^6}$.

It is clear that a uniform thickness and density disk is obtained by setting $\alpha=0$ in Eq. (1) and $r=0$ in Eq. (2), respectively. In this work, an elastic–linear hardening [2] model is used for modeling the stress–strain behavior of the disk material:

$$\begin{cases}\varepsilon=\dfrac{\sigma}{\mathrm{E}} & \sigma\le\sigma_\circ\\ \varepsilon=\dfrac{\sigma_\circ}{\mathrm{E}}+\dfrac{1}{\mathrm{E}_t}(\sigma-\sigma_\circ) & \sigma\langle\sigma_\circ\end{cases} \tag{3}$$

where $\sigma_\circ$ and E_t are the yield strength of the material and tangent modulus, respectively. Table 1 shows the geometry and material properties used for the disks studied in this research.

Table 1
Geometry and material properties and angular velocity constant of rotating disks.

Outer radius of disk	$r_e\,(m)$	0.8
Inner radius of disk	$r_i\,(m)$	0.1
Thickness at $r=r_e$	$h_0\,(m)$	0.1
Young's modulus	$E\,(GPa)$	200
Poisson's ratio	υ	0.3
Shear modulus	$G\,(GPa)$	77
Tangent modulus	$E_t\,(GPa)$	80
Yield strength of material	$\sigma_\circ\,(MPa)$	300

3 THEORETICAL BACKGROUND

3.1 Governing equation of rotating disk

In this section, assuming that the disk is thin, having a variable thickness which is a function of r , and it is rotating with a constant angular acceleration, around the z-axis. Fig.3 shows an element of the disk with all in-plane tractions in the radial (r) and tangential (θ) directions of coordinate system located at the center of the disk. The equations of equilibrium in relative directions can be indicated as [1, 2]:

$$\frac{d}{dr}\left[\sigma_r h(r) r\right]+\frac{d\tau_{r\theta}}{d\theta}h(r)-\sigma_\theta h(r)=-\rho(r)\omega^2 r^2 h(r) \tag{4}$$

$$\frac{d}{dr}\left[\tau_{r\theta} h(r) r\right]+\tau_{r\theta} h(r)=-\rho(r)\dot{\omega} r^2 h(r) \tag{5}$$

where, $\rho(r)$ is the distribution function of density, ω is the angular velocity and $\dot{\omega}$ is the angular acceleration of the disk. Otherwise, σ_r and σ_θ are radial and tangential components of the normal stresses and $\tau_{r\theta}$ is the in-plane shear stress. Due to the rotational symmetry of the problem, displacements fields are functions of r only and Eqs. (4-5) can be further simplified to:

$$\frac{d}{dr}\left[\sigma_r h(r) r\right]-\sigma_\theta h(r)=-\rho(r)\omega^2 r^2 h(r) \tag{6}$$

$$\frac{d}{dr}\left[\tau_{r\theta}(r) h(r) r\right]+\tau_{r\theta}(r) h(r)=-\rho(r)\dot{\omega} r^2 h(r) \tag{7}$$

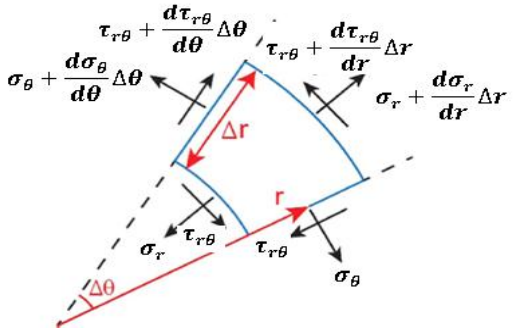

Fig.3
Acting forces on an element of disk.

In the plane stress and small deflection condition assumed for this analysis, the stress-strain relations are [2]:

$$\sigma_r(r)=\frac{E}{1-\nu^2}[\varepsilon_r(r)+\nu\,\varepsilon_\theta(r)] \tag{8}$$

$$\sigma_\theta(r)=\frac{E}{1-\nu^2}[\varepsilon_\theta(r)+\nu\,\varepsilon_r(r)] \tag{9}$$

$$\tau_{r\theta}(r)=G\gamma_{r\theta} \tag{10}$$

and the strain-displacement relations after considering the rotational symmetry condition can be presented as [2]:

$$\varepsilon_r(r)=\frac{du_r(r)}{dr} \tag{11}$$

$$\varepsilon_\theta(r)=\frac{u(r)}{r}+\frac{1}{r}\frac{du_\theta(r)}{d\theta}\xrightarrow{Rotational\ \ symmetry}\varepsilon_\theta(r)=\frac{u(r)}{r} \tag{12}$$

$$\gamma_{r\theta}(r)=\frac{1}{r}\frac{du(r)}{d\theta}+\frac{du_\theta(r)}{dr}-\frac{u_\theta(r)}{r}\xrightarrow{Rotational\ \ symmetry}\gamma_{r\theta}(r)=\frac{du_\theta(r)}{dr}-\frac{u_\theta(r)}{r} \tag{13}$$

with substitution of Eqs. (8-10 and 11-13) in relations (6 and 7), yields the following governing equation in the term of radial (u_r) and tangential (u_θ) displacements in relative direction:

$$\frac{d^2u_r(r)}{dr^2}+\left[\frac{1}{r}+\frac{1}{h(r)}\frac{dh(r)}{dr}\right]\frac{du_r(r)}{dr}-\left[\frac{1}{r^2}-\frac{\upsilon}{h(r)r}\frac{dh(r)}{dr}\right]u_r(r)=-\frac{(1-\upsilon^2)\rho(r)\omega^2 r}{E} \tag{14}$$

$$\frac{d^2u_\theta(r)}{dr^2}+\left[\frac{1}{r}+\frac{1}{h(r)}\frac{dh(r)}{dr}\right]\frac{du_\theta(r)}{dr}-\left[\frac{1}{r^2}+\frac{1}{h(r)r}\frac{dh(r)}{dr}\right]u_\theta(r)=-\frac{\rho(r)\omega^{\circ}r}{G} \tag{15}$$

where, G is shear modulus and υ is a poisson ratio. Many researchers have studied eq. (14) and hence only Eq. (15) investigated here. For mention, in references [10, 12], it has been shown that the semi-exact solution of the Eq. (14) by HPM, VIM,ADM and Runge-Kutta method are in excellent agreement for thickness and density profile $h(r)=h_\circ(\frac{r}{b})^{-n}\Big|_{0<n<1}$, $\rho(r)=\rho_\circ(\frac{r}{b})^{m}\Big|_{0<m<1}$. In this study, new thickness and density profiles are assumed; HPM and ADM are implemented for solving equilibrium Eqs. (15).

3.2 Homotopic perturbation method (HPM) [12]

Let us consider the following differential equation and boundary condition for presenting HPM [25-29]:

$$A(u)-f(r)=0,\qquad r\in\Theta, \tag{16}$$

$$B(u,\partial u/\partial n)=0,\qquad r\in\Gamma, \tag{17}$$

In this relations, u is the unknown function, A is a general differential operator, B is a boundary operator, $f(r)$ is a known analytic functional, and Γ is the boundary of the domain Θ. One of the most important steps in solving differential equation by HPM is to find the linear and nonlinear parts of the function A. Therefore in Eq. (16) function A can be separated into two parts L and N. In this definition, L is a linear part whereas N is a nonlinear part. Then, Eq. (16) can be rewritten as:

$$L(u)+N(u)-f(r)=0. \tag{18}$$

Homotopic perturbation structure is created as the following equation:

$$H(v,p)=L(v)-L(u_\circ)+pL(u_\circ)+p[N(v)-f(r)]=0 \tag{19}$$

where$v$ is a characteristic variable in HPM by below definition:

$$v(r,p):\Theta\times[0,1]\to R \tag{20}$$

In Eq. (19), $p\in[0,1]$ is an embedding parameter and $u_\circ$ is the first approximation that satisfies the boundary condition in Eq. (17).For $p=0$ and $p=1$, Eq. (19) reduces to the following equations respectively:

$$H(v,0)=L(v)-L(u_{\circ})=0\ ,\quad H(v,\ 1)=A(v)-f\ (r)=0 \tag{21}$$

This relation shows that $L(v)=L(u_{\circ})$ and $A(v)=f\ (r)$. This information is used to write Eq. (19). To start solving process, Eq. (19) is arranged according to the different powers of *p*-terms ($p^0, p^1, p^2, \ldots..$). Each coefficient of *p*-terms is a differential equation in term of variable v that must be solved. After this stage, the process of changes in *p* from zero to unity is that of $v\ (r,p)$ changing from $u_{\circ}$ to $u(r)$ .We consider *v*, as following:

$$v\ =v_0+pv_1+p^2v_2+p^3v_3+.... \tag{22}$$

In addition, the best approximation for solution is:

$$u=\lim_{p\to 1}\ v\ \ =v_{\circ}+v_1+v_2+..... \tag{23}$$

The above convergence is discussed in [26-30].

3.3 Adomian's decomposition method [12]

In order to begin the FDM, general form of differential equation must be considered as $Fu=g$. In this relation, *u* is the unknown function and at the end of ADM algorithm its change function must be calculated. Also *F* represents a general nonlinear differential operating consisting of both linear and nonlinear terms of unknown variable *u*. Moreover, the *g* function is part of the differential equation where the unknown variable u does not exist. The linear terms are further decomposed to $L+R$, where L is easily invertible (usually the highest-order derivative) and R is the remaining terms of linear operator. The nonlinear term is represented by *N*. The general equation of $Fu=g$ now can be rewritten as [30-32]:

$$Lu+Nu+Ru=g \tag{24}$$

The nonlinear operator $[Nu]$ can be decomposed by an infinite series of polynomials given by,

$$Nu=\sum_{n=0}^{\infty}A_n(u_0,u_1,\ldots.,u_n) \tag{25}$$

where $A_n(u_0,u_1,\ldots.,u_n)$ are the appropriate Adomian's polynomials defined by,

$$A_n=\frac{1}{n!}[\frac{d^n}{d\lambda^n}N(\sum_{k=0}^{\infty}\lambda^k u_k)],n\geq 0 \tag{26}$$

Assuming that the inverse operator L^{-1} exists and it can be taken as the definite integral with respect to r from r_0 to r ,

$$L^{-1}=\int_{r_0}^{r}(.)dr \tag{27}$$

If *L* is a second-order operator, L^{-1} is a twofold indefinite integral,

$$L^{-1}Lu=u-u\ (0)-r\frac{\delta u(0)}{\delta r} \tag{28}$$

Solving Eq. (24) for *Lu* and multiplying L^{-1} on both sides gives:

$$L^{-1}Lu = L^{-1}g - L^{-1}(Ru) - L^{-1}(Nu) \tag{29}$$

Comparing Eqs. (28) and (29) gives:

$$u = f(r) - L^{-1}(Ru) - L^{-1}(Nu) \tag{30}$$

where

$$f(r) = f_1(r) + f_2(r) \tag{31}$$

Just as seen in Eq. (31), $f(r)$ is decomposed to two parts: $f_1(r)$ and $f_2(r)$. $f_1(r)$ is the part corresponding to the function g in original differential equation and $f_2(r)$ arises from the prescribed initial or boundary conditions. The standard Adomian method defines the solution $u(r)$ by the series:

$$u(r) = \sum_{n=0}^{\infty} u_n(r) \tag{32}$$

where the components $u_0, u_1, u_2, \ldots$ are usually determined by using recursive relation:

$$\begin{aligned} &u_0(r) = f(r) \\ &u_{n+1}(r) = -L^{-1}(Ru_n) - L^{-1}(Nu_n), n \geq 0 \end{aligned} \tag{33}$$

with this relation, the components of $u_n(r)$ are easily obtained. This leads to the solution in a series form. The solution in a closed form follows immediately if an exact solution exists [30-32].

3.4 Finite difference method (FDM) [16]

Finite difference method is one of the effective methods for numerical solution of differential equations. This method is one of the simplest and the oldest method to solve differential equations that are difficult or impossible to solve. The approximation of derivatives by finite difference plays a central role in FDM for numerical solution of differential equation. The accuracy of the solution depends on the chosen number of grid points. One can increase the accuracy of the solution to some desired degree by increasing the number of grid points. To solve differential equations with specified boundary conditions, we need to define a set of grid points in the variables interval that is divided into $N-1$ equal or non-equal parts. The derivatives of a function $f(r)$ are always approximated by central difference equations. However, derivatives for grid point in boundary conditions are written on the base of forward and backward finite difference form. Therefore, the firs derivative with respect to r in central-forward-backward difference form can be written as [34-35]:

$$\begin{aligned} &\left.\frac{df}{dr}\right|^{r=r_i} \xrightarrow{Central} \frac{f^{i+1} - f^{i-1}}{2\delta_r} + O(h^2) \\ &\left.\frac{df}{dr}\right|^{r=r_i} \xrightarrow{Forward} \frac{f^{i+1} - f^{i}}{\delta_r} + O(h) \\ &\left.\frac{df}{dr}\right|^{r=r_i} \xrightarrow{Backward} \frac{f^{i} - f^{i-1}}{\delta_r} + O(h) \end{aligned} \tag{34}$$

while the second derivative of a function $f(r)$ with respect to *r* is:

$$\left.\frac{d^2f}{dr^2}\right|_{r=r_i} \xrightarrow{Central} = \frac{f^{i+1}-2f^{i}+f^{i-1}}{\delta_r^{\,2}}+O(h^2)$$
$$\left.\frac{d^2f}{dr^2}\right|_{r=r_i} \xrightarrow{Forward} = \frac{f^{i+2}-2f^{i+1}+f^{i}}{\delta_r^{\,2}}+O(h) \tag{35}$$
$$\left.\frac{d^2f}{dr^2}\right|_{r=r_i} \xrightarrow{Backward} = \frac{f^{i}-2f^{i-1}+f^{i-2}}{\delta_r^{\,2}}+O(h)$$

Other finite difference forms of derivatives for a function $f(r)$ are available in the references [34-35]. For each grid point in the interval [0,1], the differential equation is written in the finite difference form. In addition, the boundary conditions are written in this scheme. Finally, the set of linear algebraic equations can be obtained in the following matrix expression that must be solved using an appropriate method [35].

$$A \cdot U = B \tag{36}$$

For annular rotating disk finite difference scheme in radial direction and numbering of grid point are constructed as shown in Fig.4. At the end of the finite difference process, there are $N-2$ equations for the inner points and two equations for the inner and outer surface boundary condition of the disk.

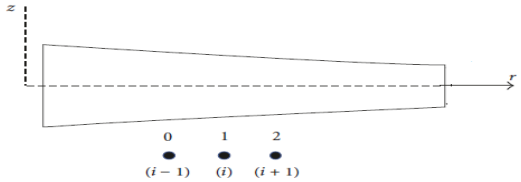

Fig.4
Finite difference scheme in radial direction of rotating disk.

4 SEMI_ EXACT SOLUTION

In this section, we consider elastic annular rotating disks with variable thickness and density, under variable mechanical loading. Based on the goals of paper, the equilibrium equation in tangential direction (Eq. (15)) is solved.

4.1Application of HPM

To use HPM, Eqs. (1-2) are substituted into Eq. (15) and yields the following differential equation in term of unknown tangential displacement:

$$\frac{d^2u_\theta(r)}{dr^2}+\left[\frac{(1+\alpha)}{r}\right]\frac{du_\theta(r)}{dr}-\left[\frac{(1+\alpha)}{r^2}\right]u_\theta(r)=-\frac{(\rho_0+\rho_1 r+\rho_2 r^2+\rho_3 r^3)\omega^2 r}{G} \tag{37}$$

After separating the linear and nonlinear parts of this equation according to descriptions for Eq. (19), HPM can be applied as:

$$L(v)=\frac{d^2v(r)}{dr^2}+\left[\frac{(1+\alpha)}{r}\right]\frac{dv(r)}{dr}-\left[\frac{(1+\alpha)}{r^2}\right]v(r) \tag{38}$$

$$L(u_{0\theta})=\frac{d^2u_{0\theta}(r)}{dr^2}+\left[\frac{(1+\alpha)}{r}\right]\frac{du_{0\theta}(r)}{dr}-\left[\frac{(1+\alpha)}{r^2}\right]u_{0\theta}(r) \tag{39}$$

$$f(r)=-\frac{(\rho_0+\rho_1 r+\rho_2 r^2+\rho_3 r^3)\omega^2 r}{G} \tag{40}$$

where $L(v)$ is the linear part of the Eq. (37) and $L(u_{0\theta})$ is its initial approximation. With substituting Eqs. (38-40) into Eq. (19) and rearranging based on powers of *p*-terms, we have:

$$p^0: \frac{u_{0\theta}(r)}{r^2}-\frac{du_{0\theta}(r)}{dr}\frac{\alpha}{r}+\frac{dv_0(r)}{dr}\frac{1}{r}-\frac{d^2u_{0\theta}(r)}{dr^2}-\frac{\alpha v_0(r)}{r^2}+\frac{d^2v_0(r)}{dr^2}-\frac{v_0(r)}{r^2}-\frac{du_{0\theta}(r)}{dr}\frac{1}{r}+\frac{\alpha u_{0\theta}(r)}{r^2}+\frac{dv_0(r)}{dr}\frac{\alpha}{r}=0 \tag{41}$$

$$p^1: -\frac{u_{0\theta}(r)}{r^2}+\frac{d^2v_1(r)}{dr^2}+\frac{d^2u_{0\theta}(r)}{dr^2}+\frac{du_{0\theta}(r)}{dr}\frac{1}{r}-\frac{\alpha v_1(r)}{r^2}+\frac{dv_1(r)}{dr}\frac{\alpha}{r}-\frac{v_1(r)}{r^2}+\frac{dv_1(r)}{dr}\frac{1}{r}-\frac{\alpha u_{0\theta}(r)}{r^2}+\frac{du_{0\theta}(r)}{dr}\frac{\alpha}{r}$$
$$+\frac{(\rho_0+\rho_1 r+\rho_2 r^2+\rho_3 r^3)\omega^{\circ} r}{G}=0 \tag{42}$$

$$p^2: \frac{dv_2(r)}{dr}\frac{1}{r}-\frac{\alpha v_2(r)}{r^2}+\frac{d^2v_2(r)}{dr^2}-\frac{v_2(r)}{r^2}+\frac{dv_2(r)}{dr}\frac{\alpha}{r}=0 \tag{43}$$

To determine *v* function, the above equations are to be solved. Solving Eq. (41), we have:

$$v_0(r)=u_{0\theta}(r)=C_1 r+C_2 r^{(-\alpha-1)} \tag{44}$$

Similarly solving Eqs. (42 - 43) yields the following results respectively:

$$v_1(r)=C_1 r+C_2 r^{(-\alpha-1)}+\frac{1}{60}\frac{\omega^{\circ} r^3}{(-\alpha-4)(-\alpha-5)(-\alpha-6)(-\alpha-7)G}$$
$$[\left(-6300-3210\alpha-540\alpha^2-30\alpha^3\right)\rho_0+\left(-3360-1880\alpha-340\alpha^2-20\alpha^3\right)r\rho_1$$
$$+\left(-2100-1245\alpha-240\alpha^2-15\alpha^3\right)r^2\rho_2+\left(-1440-888\alpha-180\alpha^2-12\alpha^3\right)r^3\rho_3] \tag{45}$$

$$v_2(r)=C_1 r+C_2 r^{(-\alpha-1)} \tag{46}$$

Substitution of the above Eqs. (44-46) in Eq. (22) gives the equation for *v* and as $p \xrightarrow{yields} 1$, then $v \xrightarrow{yields} u_{\theta}$. This means finding the answer for the governing equation of elastic rotating disk (i.e., Eq. (15)) in the general form of non-uniform thickness and density. The optimum number of HPM iteration considering the converged result is two. Therefore, the exact solution of $u_{\theta}(r)$ is:

$$u_{\theta}(r)=v_0(r)+pv_1(r)+p^2v_2(r)\big|_{p=1}=C_1 r+C_2 r^{(-\alpha-1)}+\frac{1}{60}\frac{\omega^{\circ} r^3}{(-\alpha-4)(-\alpha-5)(-\alpha-6)(-\alpha-7)G}$$
$$[\left(-6300-3210\alpha-540\alpha^2-30\alpha^3\right)\rho_0+\left(-3360-1880\alpha-340\alpha^2-20\alpha^3\right)r\rho_1$$
$$+\left(-2100-1245\alpha-240\alpha^2-15\alpha^3\right)r^2\rho_2+\left(-1440-888\alpha-180\alpha^2-12\alpha^3\right)r^3\rho_3] \tag{47}$$

In this relation, C_1 and C_2 are integrations constant to be determined by applying boundary conditions of rotating disk at inner and outer surfaces. In this paper, two different types of boundary conditions are considered. These conditions are explained in details in the next sections.

4.2 Application of ADM

The general governing Eq. (37) for an elastic rotating disk with variable thickness, density and angular velocity, has to be solved with the initial condition. The best zeroth approximation is obtained by assuming $f_1(r)$ and $f_2(r)$ as follows:

$$f_1(r)=L_{rr}^{-1}\left(g(r)\right)=-\frac{\omega^{\circ}\left(\frac{1}{30}\rho_3 r^6+\frac{1}{20}\rho_2 r^5+\frac{1}{12}\rho_1 r^4+\frac{1}{6}\rho_0 r^3\right)}{G}$$
$$f_2(r)=C_1 r+C_2 r^{(-\alpha-1)} \tag{48}$$

As seen in Eq. (48), one of the ways to find the function $f_2(r)$ is to consider it equal to the first approximation ($u_{0\theta}(r)$ in Eq. (44)) obtained by the HPM. Now initial approximation by ADM can be presented as:

$$u_{0\theta}(r)=f_1(r)+f_2(r)=C_1 r+C_2 r^{(-\alpha-1)}-\frac{\omega^{\circ}\left(\frac{1}{30}\rho_3 r^6+\frac{1}{20}\rho_2 r^5+\frac{1}{12}\rho_1 r^4+\frac{1}{6}\rho_0 r^3\right)}{G} \tag{49}$$

By the same manner, other components of $u_{\theta}(r)$ are found. The optimum number of ADM iteration considering the converged result is three.

$$u_{1\theta}(r)=-L_{rr}^{-1}\left(\left(\frac{(1+\alpha)}{r}\right)\frac{du_{0\theta}(r)}{dr}\right)-L_{rr}^{-1}\left(-\left(\frac{(1+\alpha)}{r^2}\right)u_{0\theta}(r)\right)=$$
$$\frac{1}{3600G}\begin{pmatrix}(1+\alpha)20r^6\rho_3\omega^{\circ}+(1+\alpha)36r^5\rho_2\omega^{\circ}+(1+\alpha)75r^4\rho_1\omega^{\circ}\\+(1+\alpha)200r^3\rho_0\omega^{\circ}+3600C_2r^{-\alpha-1}G\end{pmatrix} \tag{50}$$

and,

$$u_{2\theta}(r)=-L_{rr}^{-1}\left(\left(\frac{(1+\alpha)}{r}\right)\frac{du_{1\theta}(r)}{dr}\right)-L_{rr}^{-1}\left(-\left(\frac{(1+\alpha)}{r^2}\right)u_{1\theta}(r)\right)=$$
$$\frac{1}{216000G}\begin{pmatrix}(-2\alpha-\alpha^2-1)200r^6\rho_3\omega^{\circ}+(-2\alpha-\alpha^2-1)432r^5\rho_2\omega^{\circ}\\+(-2\alpha-\alpha^2-1)1125r^4\rho_1\omega^{\circ}+(-2\alpha-\alpha^2-1)4000r^3\rho_0\omega^{\circ}+216000C_2r^{-\alpha-1}G\end{pmatrix} \tag{51}$$

and,

$$u_{3\theta}(r)=-L_{rr}^{-1}\left(\left(\frac{(1+\alpha)}{r}\right)\frac{du_{1\theta}(r)}{dr}\right)-L_{rr}^{-1}\left(-\left(\frac{(1+\alpha)}{r^2}\right)u_{1\theta}(r)\right)=$$
$$\frac{1}{12960000G}\begin{pmatrix}(3\alpha+3\alpha^2+\alpha^3+1)2000r^6\rho_3\omega^{\circ}+(3\alpha+3\alpha^2+\alpha^3+1)5184r^5\rho_2\omega^{\circ}\\+(3\alpha+3\alpha^2+\alpha^3+1)16875r^4\rho_1\omega^{\circ}+(3\alpha+3\alpha^2+\alpha^3+1)80000r^3\rho_0\omega^{\circ}+12960000C_2r^{-\alpha-1}G\end{pmatrix} \tag{52}$$

Therefore, the solution of Eq. (37) by ADM is,

$$\begin{aligned}u_{\theta}(r)=\sum_{n=0}^{3}u_{n\theta}(r)=u_{0\theta}(r)+u_{1\theta}(r)+u_{2\theta}(r)+u_{3\theta}(r)&=C_1r+C_2r^{(-\alpha-1)}-\frac{1}{G}\omega^{\circ}\left(\frac{1}{30}\rho_3r^6+\frac{1}{20}\rho_2r^5+\frac{1}{12}\rho_1r^4+\frac{1}{6}\rho_0r^3\right)\\&+\frac{1}{3600G}\begin{pmatrix}(1+\alpha)20r^6\rho_3\omega^{\circ}+(1+\alpha)36r^5\rho_2\omega^{\circ}+(1+\alpha)75r^4\rho_1\omega^{\circ}\\+(1+\alpha)200r^3\rho_0\omega^{\circ}+3600C_2r^{-\alpha-1}G\end{pmatrix}\\&+\frac{1}{216000G}\begin{pmatrix}(-2\alpha-\alpha^2-1)200r^6\rho_3\omega^{\circ}+(-2\alpha-\alpha^2-1)432r^5\rho_2\omega^{\circ}\\+(-2\alpha-\alpha^2-1)1125r^4\rho_1\omega^{\circ}+(-2\alpha-\alpha^2-1)4000r^3\rho_0\omega^{\circ}+216000C_2r^{-\alpha-1}G\end{pmatrix}\\&+\frac{1}{12960000G}\begin{pmatrix}(3\alpha+3\alpha^2+\alpha^3+1)2000r^6\rho_3\omega^{\circ}+(3\alpha+3\alpha^2+\alpha^3+1)5184r^5\rho_2\omega^{\circ}\\+(3\alpha+3\alpha^2+\alpha^3+1)16875r^4\rho_1\omega^{\circ}+(3\alpha+3\alpha^2+\alpha^3+1)80000r^3\rho_0\omega^{\circ}+12960000C_2r^{-\alpha-1}G\end{pmatrix}\end{aligned} \tag{53}$$

5 NUMERICAL SOLUTION

5.1 Application of FDM

The differential Eq. (15) is valid for elastic deformations of non-uniform thickness and density rotating disk under variable angular velocity as mechanical loading in tangential direction. To solve the differential equation by finite difference method, derivatives of tangential displacement component in the radial direction are to be replaced by Eqs. (34-35). Finally, the finite difference form of the differential equation is expressed as follow:

$$\frac{u_\theta{}^{i+1}-2u_\theta{}^{i}+u_\theta{}^{i-1}}{\delta_r^2}+\frac{(1+\alpha)}{r_i}\frac{u_\theta{}^{i+1}-u_\theta{}^{i-1}}{2\delta_r}-\frac{(1+\alpha)}{r_i{}^2}u_\theta{}^{i}=-\frac{\left(\rho_0+\rho_1 r_i+\rho_2 r_i{}^2+\rho_3 r_i{}^3\right)\omega^{\circ}{}_i r_i}{G} \tag{54}$$

The radial direction of the disk ($r\epsilon[r_i,r_o]$) is divided to N grid points ($i=[1,N]$). For internal grid points ($i=[2,N-1]$), the FD form of differential Eq. (54) is written. In addition, the boundary condition of the rotating disk at the inner and outer surfaces of the disk must be expressed in FD form. In this paper two different boundary conditions is considered and the FD form of them are as follow:

(a) Radially constrained and guided boundary conditions: if the inner surface of the annular disk is mounted on a rigid shaft and outer surface is guided as shown in Fig. 1, then the boundary conditions and the FD form of this boundary conditions are:

$$\begin{cases} i=1, u_\theta(r_i)=0 \quad \underrightarrow{yields} \quad u_\theta^i=0 \\ i=N, u_\theta(r_e)=0 \quad \underrightarrow{yields} \quad u_\theta^i=0 \end{cases} \tag{55}$$

(b) Radially constrained and free boundary conditions: if the annular disk is mounted on a rigid shaft and outer surface is free of any traction, boundary conditions and the FD form of this boundary conditions are:

$$\begin{cases} i=1, \quad u_\theta(r_i)=0 \quad \underrightarrow{yields} \quad u_\theta^i=0 \\ i=N, \tau_{r\theta}(r_e)=0 \quad \underrightarrow{yields} \quad \frac{1}{G}\left(\frac{du_\theta(r)}{dr}-\frac{u_\theta(r)}{r}\right)=0 \quad \underrightarrow{yields} \quad \frac{u_\theta^i-u_\theta^{i-1}}{\delta_r}-\frac{u_\theta^i}{r_i}=0 \end{cases} \tag{56}$$

Finally, a system of linear algebraic equations is obtained. By solving the system of equations, the tangential displacement of the rotating disk for each grid point is calculated.

6 RESULTS AND DISCUSSIONS

Table 1 records the geometry and material properties used for disks studied in this research. The main aim of this section is to demonstrate the ability of the HPM and ADM to handle non-uniform thickness and density rotating disks, with considering variable angular velocity in current simulations. Because of its fast rate of convergence, these methods are particularly suitable for nonlinear problems. It is quite interesting to notice that the exact solution of the Eq. (15) for uniform thickness and density rotating disk in tangential direction can be shown as [36]:

$$u_\theta(r)=\frac{C_1}{2Gr}-C_2 r-\frac{\rho\omega^{\circ}r^3}{8G} \tag{57}$$

The constants C_1 and C_2 in this equation are determined by applying boundary conditions. As mentioned earlier, two different boundary conditions are applied on the annular disk.

In Finite difference method and for solving equilibrium equation in FD form as Eq. (54), in order to increase the accuracy of the solutions, the radial distance, (r_e-r_i), is divided into N steps, $\delta_r=\frac{(r_e-r_i)}{N}$. Moreover, a mesh sensitivity analysis was performed to ensure that the results are not dependent on the mesh size, and N was set to 401.

For the uniform thickness and density case, Fig.5 compares the HPM, ADM and FDM results for tangential displacement and shear stress with radially constrained-free boundary condition with those results obtained from exact solution as Eq. (57)[16]. Fig. 6 compares these results for radially constrained-guided boundary condition. With considering the performance of disks used in actual work environments, an angular acceleration ($\omega^{\circ}=100\pi\, rad/s^2$) is considered. For this value of angular acceleration, the displacement in rotating disk is in an elastic region. As it can be seen in these figures, the agreement between the results of HPM, ADM and FDM solutions for uniform disk is excellent in comparison with exact solution. As shown in Figs.5 and 6, boundary conditions are completely satisfied. For radially constrained-free condition, the shear stress is reaches its maximum value at inner surface ($r=r_i$). However, for radially constrained-guided condition maximum value of shear stress occurs at both inner and outer surface of disk. In this boundary condition, shear stress at inner surface is positive and at outer surface of disk is negative. Along the radial direction of this disk, there is a point in which shear stress is zero. The level of displacement and stress in disk with this boundary condition is much less than radially constrained-free condition. This means that elastic limit of the angular velocity at which yielding begins for disk with constrained-guided boundary condition is less than disk with constrained-free boundary condition.

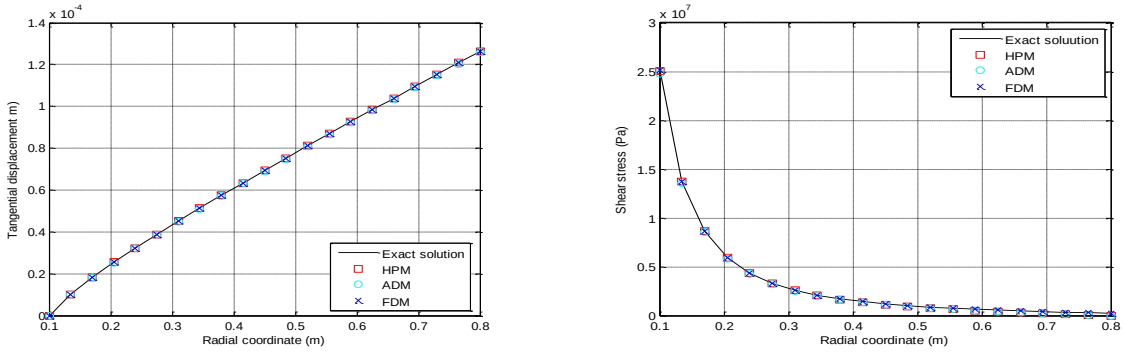

(a) (b)

Fig.5
Comparison of results for rotating an annular disk with radially constrained-free conditions, uniform thickness and density: (a) tangential displacement and (b) shear stress.

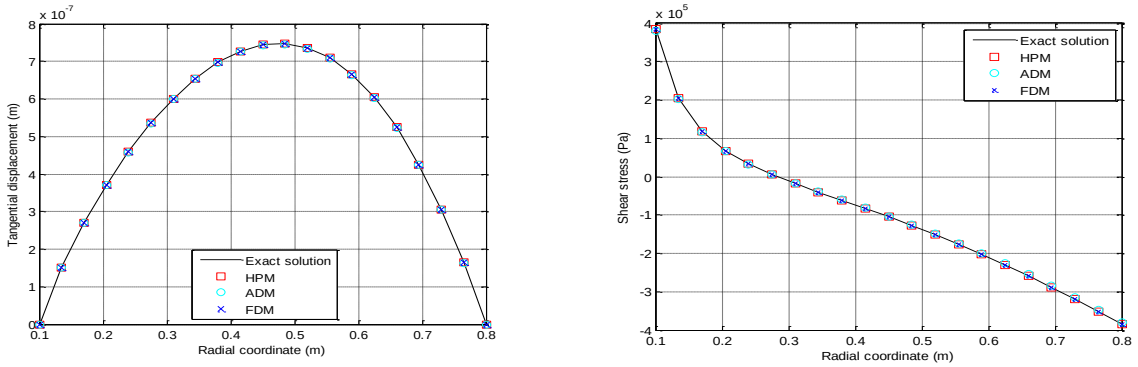

(a) (b)

Fig.6
Comparison of results for rotating an annular disk with radially constrained-guided conditions, uniform thickness and density: (a) tangential displacement and (b) shear stress.

For non-uniform thickness and density case, in order to verifying HPM and ADM results for tangential displacement and shear stress, different thickness parameter based on the definitions in Eq. (1) is selected ($\alpha=-0.5$ and $\alpha=0.5$). The results are compared with FDM solution in Figs. 7 and 8 for two prescribed boundary conditions. All the presented results are based on using a constant angular acceleration ($\omega^{\circ}=100\pi\, rad/s^2$) and density function according to Eq. (2). It is important to note that rotating disks with non-uniform thickness and density have no exact solution. These figures show the ability of these methods to solve the governing equation of rotating disk in its

general form. In HPM, two iteration leads to high accuracy of the solution for the governing equation of the problem in its general form (non-uniform thickness and density). This solution is in good agreement with the exact and FDM results. In ADM case, non-uniform solution after three iterations and much more calculations than HPM is obtained. Optimum identification of initial conditions for ADM is difficult and one way to find it is use special terms of HPM solution. Comparison between HPM and ADM shows that although the results of these semi-exact methods when applied to the elastic equation in annular disks are the same approximately, but HPM does not require specific algorithms, complex calculations and high computational size such as ADM and is much easier and more convenient than ADM.

As seen in Figs. 7 and 8, when non-uniform thickness and density is considered, the level of tangential displacement and shear stress at every affected point of the disk with constrained-free conditions is decreases for $\alpha = -0.5$ and increases for $\alpha = 0.5$ in compared to uniform disk with $\alpha = 0$. Moreover, these conditions in disk with constrained-guided boundary are different. In disk with this kind of boundary conditions, level of displacement is decreases for $\alpha = 0.5$ and increases for $\alpha = -0.5$ in compared to disk with $\alpha = 0$. In the case of shear stress as shown in the Fig. 8, level of shear stress on the inner and outer surface of the disk is not equal, unlike the uniform disk. At the inner surface of the disk, the disk with $\alpha = 0.5$ and at the outer surface, disk with $\alpha = -0.5$ have more shear stress than uniform disk. For mention, the thickness of disk decreases parabolically when $-1 \le \alpha < 0$ and varies approximately linearly when $0 < \alpha \le 1$. Based on these results, it can be said that always considering the disk with non-uniform thickness dose not reduce the displacement-stress levels in rotating disk. The factors that contribute to these results are the type of disk boundary conditions.

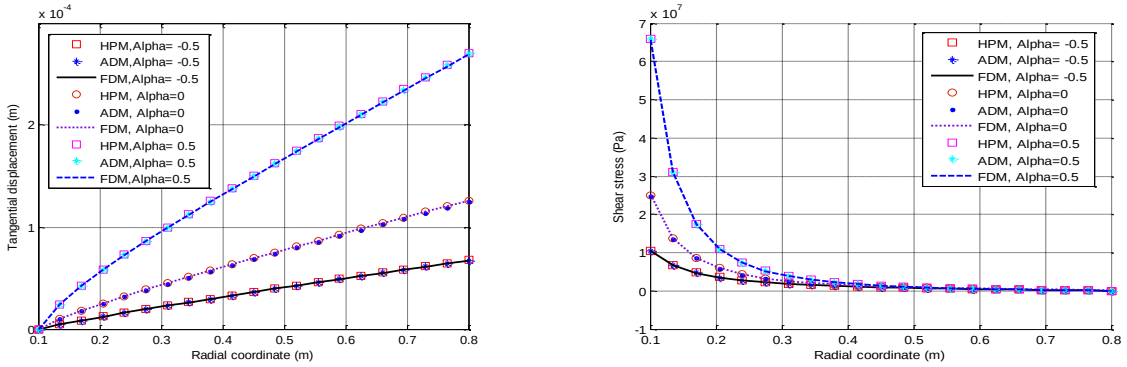

(a) (b)

Fig.7

Comparison of results for rotating an annular disk with constrained-free conditions, thickness parameter $\alpha = -0.5, 0, 0.5$ and density function $\rho(r)$: (a) tangential displacement, (b) shear stress.

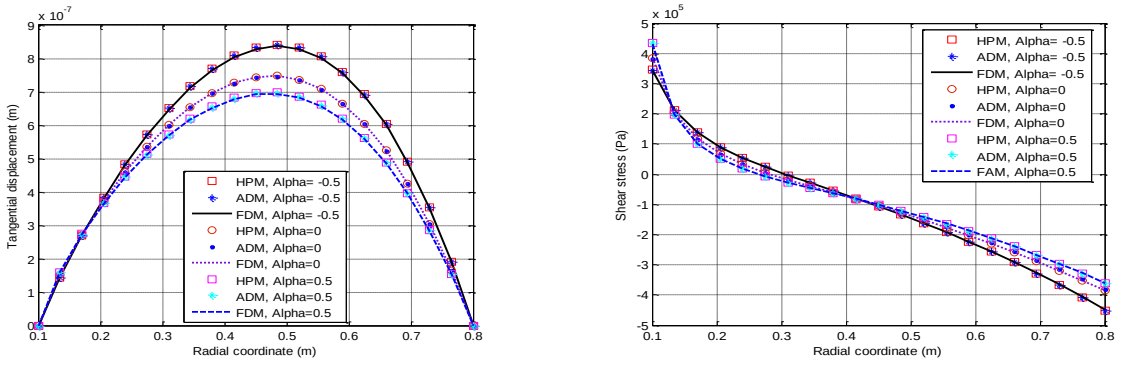

(a) (b)

Fig.8

Comparison of results for rotating an annular disk with constrained-guided conditions, thickness parameter $\alpha = -0.5, 0, 0.5$ and density function $\rho(r)$: (a) tangential displacement, (b) shear stress.

7 PARAMETRIC STUDY

The main object of this section is to carry out a parametric study on effects of the boundary conditions, the geometric parameter α and the value of angular acceleration on the behavior of the rotating disk with non-uniform thickness and density. Based on this information, the optimum disk profile is selected for prescribed boundary conditions. Firstly, variation of the tangential displacement and the shear stress for different values of α, are shown in Figs. 9 and 10. The boundary conditions of the disk are considered as constrained-free and constrained-guided in these figures, respectively. The reported results are based on using the HPM solution and angular acceleration as $(\omega^{\circ}=100\pi\, rad/s^2)$. As shown in these figures, all the results expressed in Figs. 7 and 8 for certain values of thickness parameter α can be generalized to different values of α for each boundary condition. For constrained-free condition and range of changes $-1\le\alpha<0$, as the thickness parameter increases, the level of tangential displacement along the radius of the disk decreases. Nevertheless, for range of changes $0\le\alpha<1$, as the thickness parameter increases, the level of the tangential displacement also increases. It can be seen that for both ranges of α, the tangential displacement reaches its maximum value at outer surface ($r=r_e$) in Fig. 9 and this condition approximately occurs in the middle radius of the disk in Fig. 10.

In term of the shear stress, the distribution of stress is completely different for the two boundary conditions. For constrained-free condition, shear stress reaches its maximum value at inner surface, ($r=r_e$) and as the thickness parameter increases, the level of stress decreases for $-1\le\alpha<0$ (parabolically) and increases for $0\le\alpha<1$ (linearly). However, for constrained-guided condition, it is found that the value of stress in the inner and outer surfaces of the disk is not equal. For a certain value of thickness parameter in the range $-1\le\alpha<0$, while the inner surface of the disk is thicker than outer surface, experiences lower stress. For range $0\le\alpha<1$, although the inner surface is thicker, it experiences more stress. For all values of α, as the thickness parameter becomes smaller, the thickness changes become more uniform and the difference of shear stress between the inner and outer surfaces of the disk decreases. As the thickness parameter increases, the point in which shear stress are zero moves to the middle radius of the disk for $-1\le\alpha<0$ and moves to the inner radius of disk for $0\le\alpha<1$. It can be concluded that the proposed HPM can successfully handle the problem of a rotating disk under variable mechanical loading. These results can be used to select the optimal disk profile from the point of view of tangential displacement-shear stress distribution in rotating disk. Shear stress is involved in the calculation of equivalent stress, which is a limit for plastic deformation initiation. Accordingly, the optimal disk profile for each boundary condition is as follows:

- Constrained-free condition: rotating disk with a thickness parameter $\alpha=-1$ has the least amount of tangential displacement-shear stress among different values of α.
- Constrained-guided condition: rotating disk with thickness parameter $\alpha=-1$ at inner surface and $\alpha=1$ at outer surface has the least amount of shear stress among different values of α. In term of tangential displacement, $\alpha=1$ has the least amount among different values of α.

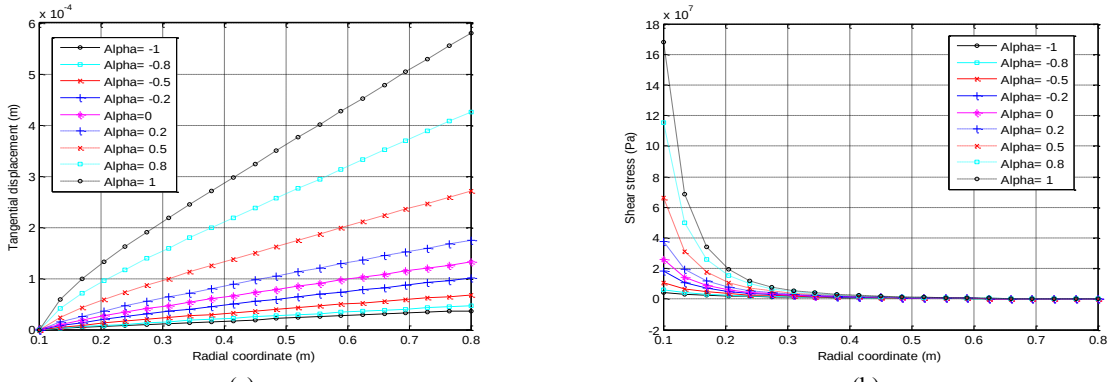

(a) (b)

Fig.9
Comparison of results for rotating an annular disk with constrained-free conditions, different thickness parameter α and density function $\rho(r)$: (a) tangential displacement, (b) shear stress.

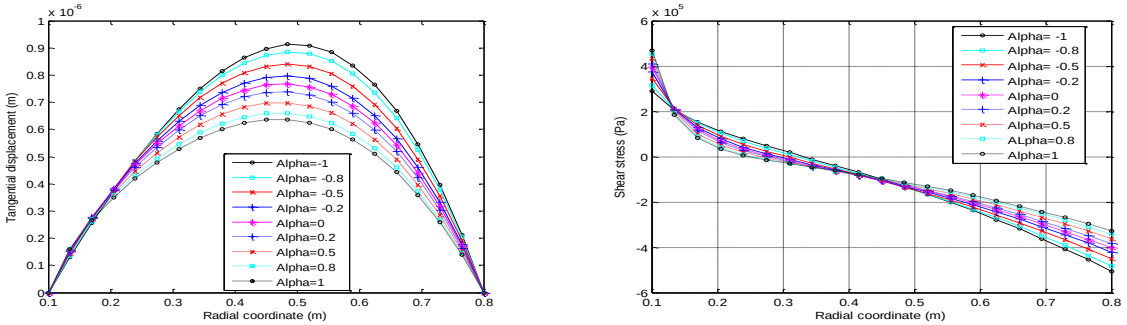

(a) (b)

Fig.10
Comparison of results for rotating an annular disk with constrained-guided conditions, different thickness parameter α and density function $\rho(r)$: (a) tangential displacement, (b) shear stress.

The variation of tangential displacement and shear stress along the radius of the disk for an arbitrary geometric parameter $\alpha = -0.5$ and different value of angular acceleration is shown in Figs. 11 and 12. As described in the previous sections, boundary conditions of the disk are considered as constrained-free and constrained-guided in these figures. The reported results are based on using the HPM and angular acceleration $(\omega^{\circ} = (50\pi, 100\pi, 150\pi)\, rad/s^2)$.

It is observed from these figures that as the angular acceleration increases, the levels of displacement and stress are increases. With increasing the angular acceleration, the rate of change of shear stress along the radius of the disk increases. From Fig. 12, it can be seen that the radial coordinate in which stress is zero remains constant for all values of angular acceleration.

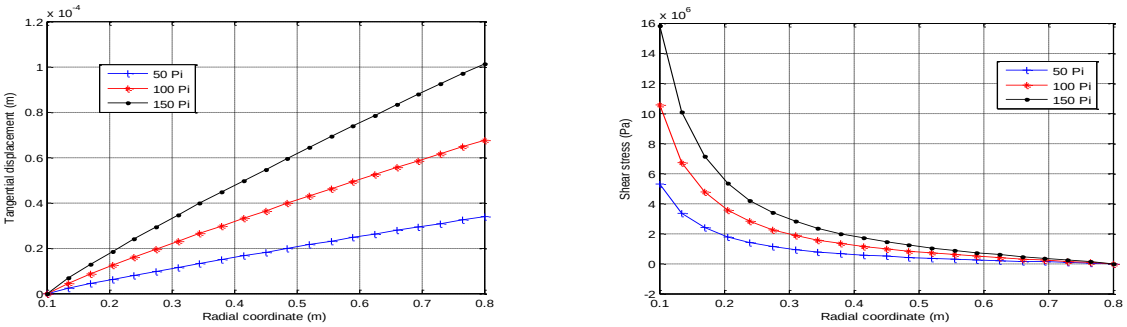

(a) (b)

Fig.11
Variation of results for rotating an annular disk with constrained-free conditions, thickness parameter $\alpha = -0.5$ and different angular acceleration: (a) tangential displacement, (b) shear stress.

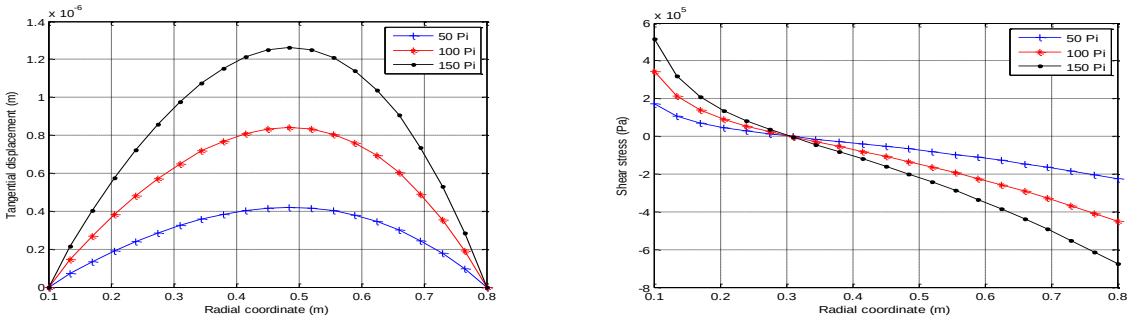

(a) (b)

Fig.12
Variation of results for rotating an annular disk with constrained-guided conditions, thickness parameter $\alpha = -0.5$ and different angular acceleration: (a) tangential displacement, (b) shear stress.

8 CONCLUSION

In this work homotopic perturbation method and adomian decomposition method as semi-exact solution methods and finite difference method as a numerical solution are used for the elastic analysis of a rotating annular disk with non-uniform thickness and density under the variable mechanical loading. HPM and ADM methods have been successfully employed to obtain the solutions of equilibrium equation of rotating disk in tangential direction. The obtained results have been compared with the FDM solution. The solutions obtained show that the results of these methods are in good agreement but HPM is easier, practical, no restriction in using and more convenient than ADM. It has been shown that the proposed methods yield accurate results without the need to use commercially available finite element analysis software. This may lead to time and cost saving in handling complicated cases. After validation, parametric studies by HPM results are done to study the elastic destructions of tangential displacement and shear stress of rotating disks under different thickness parameter, boundary conditions and angular acceleration. It is shown that boundary conditions have significant effect in reducing displacement-stress level in rotating non-uniform disk compared to uniform disk. For radially constrained-free condition, disk with parabolically thickness changing have a lower values for shear stress. But For radially constrained-guided condition, disk with parabolically thickness changing have a lower values of shear stress at inner surface of disk and disk with linearly thickness change have a lower values of shear stress at outer surface of disk. This means that with considering disk profile variable, level of displacement and stress are not always reduced and type of changing the thickness along the radius of disk and boundary condition are an important factor in this case. It can be concluded that one can analysis any arbitrary thickness function including constant, hyperbolic, exponential, or parabolic disk and density variation using semi-exact methods presented in this research.

REFERENCES

[1] Gamer U., 1984, Elastic–plastic deformation of the rotating solid disk, Ingenieur-Archiv **54**: 345-54.

[2] Guven U.,1992, Elastic–plastic stresses in a rotating annular disk of variable thickness and variable density, *International Journal of Mechanical Sciences* **43**: 1137-1153.

[3] Guven U.,1995, On the applicability of Tresca's yield condition to the linear hardening rotating solid disk of variable thickness, *ZAMM* **75**: 397-398.

[4] Guven U., 1994, The fully plastic rotating disk of variable thickness, *ZAMM* **74**: 61-65.

[5] Eraslan A.N., Orcan Y., 2002, Elastic–plastic deformation of a rotating solid disk of exponentially varying thickness, *Mechanics and Materials* **34**: 423-432.

[6] Eraslan A.N., Orcan Y., 2002, On the rotating elastic–plastic solid disks of variable thickness having concave profiles, *International Journal of Mechanical Sciences* **44**: 1445-1466.

[7] Eraslan A.N., 2002, Inelastic deformations of rotating variable thickness solid disks by Tresca's and von Mises criteria, *International Journal of Computational Engineering Science* **3**: 89-101.

[8] Eraslan A.N., Orcan Y., 2002, Von Mises yield criterion and nonlinearly hardening variable thickness rotating annular disks with rigid inclusion, *Mechanics Research Communications* **29**: 339-350.

[9] Eraslan A.N., Orcan Y., 2003, Elastic–plastic deformations of rotating variable thickness annular disks with free, pressurized and radially constrained boundary conditions, *International Journal of Mechanical Sciences* **45**: 643-667.

[10] Hojjati M.H., Jafari S., 2007, Variational iteration solution of elastic non uniform thickness and density rotating disks, *Far East Journal of Applied Mathematics* **29**: 185-200.

[11] Hojjati M.H., Hassani A., 2008, Theoretical and numerical analyses of rotating discs of non-uniform thickness and density, *International Journal of Pressure Vessels and Piping* **85**: 694-700.

[12] Hojjati M.H., Jafari S., 2008, Semi exact solution of elastic non uniform thickness and density rotating disks by homotopy perturbation and Adomian's decomposition methods Part I: Elastic Solution, *International Journal of Pressure Vessels and Piping* **85**: 871-878.

[13] Hojjati M.H., Jafari S., 2009, Semi-exact solution of non-uniform thickness and density rotating disks. Part II: Elastic strain hardening solution, *International Journal of Pressure Vessels and Piping* **86**: 307-318.

[14] HassaniA., Hojjati M.H., Mahdavi E. , Alashti R.A., Farrahi G., 2012, Thermo-mechanical analysis of rotating disks with non-uniform thickness and material properties, *International Journal of Pressure Vessels and Piping* **98**: 95-101.

[15] Jafari S., Hojjati M.H., Fathi A., 2012, Classical and modern optimization methods in minimum weight design of elastic rotating disk with variable thickness and density, *International Journal of Pressure Vessels and Piping* **92**: 41-47.

[16] Alashti R.A., Jafari S., 2016, The effect of ductile damage on plastic behavior of a rotating disk with variable thickness subjected to mechanical loading, *Scientia Iranica B* **23**: 174-193.

[17] Zheng Y., Bahaloo H., Mousanezhad D., Mahdi E., Vaziri A., Nayeb-Hashemi H., 2016, Stress analysis in functionally graded rotating disks with non-uniform thickness and variable angular velocity, *International Journal of Mechanical Sciences* **119**: 283-293.
[18] Salehian M., Shahriari B., Yousefi M., 2018, Thermo-elastic analysis of a functionally graded rotating hollow circular disk with variable thickness and angular speed, *Journal of the Brazilian Society of Mechanical Science and Engineering* **2018**: 41.
[19] Shlyannikov V. N., Ishtyryakov I. S. , 2019, Crack growth rate and lifetime prediction for aviation gas turbine engine compressor disk based on nonlinear fracture mechanics parameters, *Theoretical and Applied Fracture Mechanics* **103**: 102313.
[20] Nayak P., Bhowmick S., NathSaha K., 2019, Elasto-plastic analysis of thermo-mechanically loaded functionally graded disks by an iterative variational method, *Engineering Science and Technology*, *an International Journal* **23**: 42-64.
[21] Calladine C.R., 1969, *Engineering Plasticity*, Oxford, Pergamon Press.
[22] Timoshenko S., Goodier J. N., 1970, *Theory of Elasticity*, New York, McGraw-Hill.
[23] Johnson W., Mellor P.B., 1983, *Engineering Plasticity*, Chichester, UK, Ellis Horwood.
[24] Guraland U., Fenster S.k., 1995, *Advanced Strength and Applied Elasticity*, London, Prentice-Hall International.
[25] He J.H., 1999, Homotopy perturbation technique, *Computer Methods in Applied Mechanics and Engineering* **178**: 257-262.
[26] He J.H., 2003, Homotopy perturbation method: a new nonlinear analytical technique, *Applied Mathematics and Computation* **135**: 73-80.
[27] He J.H., 2004, Asymptotology by homotopy perturbation method, *Applied Mathematics and Computation* **6**: 156-591.
[28] He J.H., 2005, Limit cycle and bifurcation of nonlinear problems, *Chaos Solitons Fractals* **26**: 827-833.
[29] He J.H., 2005, Homotopy perturbation method for bifurcation of nonlinear problems, *International Journal of Nonlinear Sciences and Numerical Simulation* **6**: 207-208.
[30] Adomian G., 1983, *Stochastic Systems*, New York, Academic Press.
[31] Adomian G., 1994, *Solving Frontier Problems of Physics: The Decomposition Method*, Boston, Kluwer Academic.
[32] Wazwaz A.M., 2002, *Differential Equations: Methods and Applications*, Rotterdam, Balkema.
[33] El-Wakil S.A., Abdou M.A., 2007, New applications of adomian decomposition method, *Chaos Solitons Fractals* **33**: 513-522.
[34] Nakmura S., 1991, *Applied Numerical Methods with Software*, Prentice-Hall International Inc.
[35] Ashok K., Singh K., Bhadauria B.S., 2009, Finite difference formulae for unequal sub-intervals using lagrange's interpolation formula, *International Journal of Mathematical Analysis* **3**: 815-827.
[36] Tang S., 1970, Note on acceleration stress in a rotating disk, *International Journal of Mechanical Science* **12**: 205-207.